Published in final edited form as:
Exp Eye Res. 2013 August ; 113: 32–40. doi:10.1016/j.exer.2013.04.022.

The water permeability of lens aquaporin-0 depends on its lipid bilayer environment

Jihong Tong, **John T. Canty**, **Margaret M. Briggs**, and **Thomas J. McIntosh***
Department of Cell Biology, Duke University Medical Center, Durham, NC 27710, USA

Abstract

Aquaporin-0 (AQP0), the primary water channel in lens fiber cells, is critical to lens development, organization, and function. In the avascular lens there is thought to be an internal microcirculation associated with fluid movement. Although AQP0 is known to be important in fluid fluxes across membranes, the water permeability of this channel has only been measured in Xenopus oocytes and in outer lens cortical membranes, but not in inner nuclear membranes, which have an increased cholesterol/phospholipid ratio. Here we measure the unit water permeability of AQP0 in different proteoliposomes with cholesterol/phospholipid ratios and external pHs similar to those found in the cortex and nucleus of the lens. Osmotic stress measurements were performed with proteoliposomes containing AQP0 and three different lipids mixtures: (1) phosphatidylcholine (PC) and phosphatidylglycerol (PG), (2) PC, PG, with 40 mol% cholesterol, and (3) sphingomyelin (SM), PG, with 40 mol% cholesterol. At pH 7.5 the unit permeabilities of AQP0 were $3.5 \pm 0.5 \pm 10^{-14}$ cm^3/s (mean ± SEM), $1.1 \pm 0.1 \times 10^{-14}$ cm^3/s, and $0.50 \pm 0.04 \times 10^{-14}$ cm^3/s in PC:PG, PC:PG:cholesterol, and SM:PG:cholesterol, respectively. For lipid mixtures at pH 6.5, corresponding to conditions found in the lens nucleus, the AQP0 permeabilities were $1.5 \pm 0.4 \times 10^{-14}$ cm^3/s and $0.76 \pm 0.03 \times 10^{-14}$ cm^3/s in PC:PG:cholesterol and SM:PG:cholesterol, respectively. Thus, although AQP0 unit permeability can be modified by changes in pH, it is also sensitive to changes in bilayer lipid composition, and decreases with increasing cholesterol and SM content. These data imply that AQP0 water permeability is regulated by bilayer lipid composition, so that AQP0 permeability would be significantly less in the lens nucleus than in the lens cortex.

Keywords

lens; water permeability; aquaporin; fiber cells; sphingomyelin; cholesterol

1. Introduction

Aquaporin (AQP) channels, specialized for the selective permeability of water across membranes driven by osmotic gradients (Agre and Kozono, 2003; Agre et al., 1993; Zeidel et al., 1994), are critical for water distribution and cell volume control. In particular, AQP0 (formerly called MIP or MIP26), the most abundant protein in lens fiber cell membranes, is important for the development and proper function of the eye lens (Al-Ghoul et al., 2003; Shiels et al., 2000; Verkman, 2003). Cataracts, the leading cause of blindness in the world, develop in humans with mutations in AQP0 (Francis et al., 2000; Varadaraj et al., 2008; Verkman, 2003) and in mice deficient in the gene for AQP0 (Shiels et al., 2001; Verkman et al., 2008). To maintain lens transparency, the fiber cell volume and water content must be

*Corresponding author. Tel.: +1 919 684 8950; fax: +1 919 681 9929. T.McIntosh@cellbio.duke.edu (T.J. McIntosh).

tightly regulated (Donaldson et al., 2009). Since the lens is avascular to prevent light scattering, volume regulation depends on an internal microcirculation, with AQP0 playing an important role (Donaldson et al., 2001, 2009; Mathias et al., 2007; Shiels et al., 2001). Thus, determination of AQP0 water permeability in conditions corresponding to those in the different layers of the lens should provide important information relevant to this lens microcirculation.

Previous measurements of AQP0 water permeability have been done either for AQP0 expressed in Xenopus oocytes (Ball et al., 2003; Chandy et al., 1997; Francis et al., 2000; Mulders et al., 1995; Nakazawa et al., 2011; Nemeth-Cahalan and Hall, 2000; Varadaraj et al., 2005, 2008, 1999) or in vesicles made from fiber cells teased from the lens cortex (Varadaraj et al., 2005, 1999). In general, these studies showed that AQP0 is indeed a water channel, but with a smaller unit permeability than other AQPs, such as AQP1 found in lens epithelial cells or AQP4 in brain (Chandy et al., 1997; Mulders et al., 1995; Varadaraj et al., 2005; Yang and Verkman, 1997). However, technical reasons have made it impossible to make water permeability measurements from membranes from the central nucleus of the lens (Varadaraj et al., 2005). Moreover, although Xenopus oocytes are effective systems for expression of many types of transport proteins including aquaporins, their plasma membranes have a very different lipid composition compared to fiber cell membranes, and recent work has shown that AQP4 permeability is a strong function of bilayer lipid composition (Tong et al., 2012).

In this paper we extend these previous studies to determine the water permeability of AQP0 incorporated into proteoliposomes of lipid compositions relevant to lens membranes. Specifically, we measure the individual channel (unit) AQP0 permeability in bi-layers containing various concentrations of cholesterol and lens phospholipids. The cholesterol/ phospholipid (C/PL) ratio is one of the largest found in biological systems (Zelenka, 1984; Li et al., 1985). Moreover, it has been found that the cholesterol/phospholipid (C/PL) ratio increases with aging (Li et al., 1987), and that there is a gradient in C/PL ratio across the lens (Borchman et al., 1996; Li et al., 1985, 1987). For example, in the bovine lens the C/PL ratio increases from about 0.6 (mol/mol) in the cortex to about 1.4 (mol/ mol) in the nucleus (Borchman et al., 1996), which are both larger than the value of C/PL of 0.3 in Xenopus oocytes plasma membranes (Hill et al., 2005). These large values of C/PL modify the physical properties and structural order of lens bilayers (Borchman et al., 1996; Lamba et al., 1993; Widomska et al., 2007).

The phospholipid composition of lens fiber cells is also different than most cell plasma membranes with respect to both headgroup type and hydrocarbon chain composition. Like most plasma membranes, fiber cell membranes contain primarily a mixture of phosphatidylcholine (PC), phosphatidylethanolamine (PE), phosphatidylserine (PS), and sphingomyelin (SM), with relatively small amounts of other phospholipids such as phosphatidylinositol (PI) and phosphatidylglycerol (PG) (Borchman et al., 1999; Borchman and Yappert, 2010; Deeley et al., 2008; Yappert et al., 2003). However, compared to most cell plasma membranes, fiber cell membranes are enriched in SM (Borchman et al., 2004; Yappert and Borchman, 2004). SM is an unusual membrane phospholipid in that it contains mostly saturated hydrocarbon chains (Estrada and Yappert, 2004; Zigman et al., 1984), whereas other membrane lipids typically contain hydrocarbon chains with at least one double bond. Moreover, the ratio of SM to other phospholipids (such as PC) is significantly larger in the lens nucleus than in the lens cortex (Borchman et al., 2004; Yappert and Borchman, 2004; Yappert et al., 2003) so that nuclear lipid hydrocarbon chains are more saturated by a factor of 4 compared to cortical lipids (Lamba et al., 1993). In terms of total phospholipid the bovine lens SM is 25 mol% in the cortex and 46 mol% in the nucleus (Borchman et al., 2004), which can be compared to 26 mol% SM found in Xenopus oocytes

plasma membranes (Hill et al., 2005). Lipid bilayer widths and elastic moduli are both much larger for SM/cholesterol bilayers than for bilayers containing monounsaturated PCs with or without cholesterol (Rawicz et al., 2008). Fiber cell membranes also contain dihydrosphingomyelin (DHSM), which is closely related structurally to SM, with the only difference being a 4,5-trans double bond in the sphingosine backbone of SM. The ratio of SM to DHSM depends on the animal; bovine lenses contain mostly SM whereas human lenses contain mostly DHSM (Borchman and Yappert, 2010; Borchman et al., 2004; Deeley et al., 2008; Yappert and Borchman, 2004; Yappert et al., 2003). Although DHSM has a higher melting temperature than the chain-matched SM (Kuikka et al., 2001; Yappert and Borchman, 2004), the areas per molecule are quite similar for these two lipids (Kuikka et al., 2001) and in this work we focus on SM.

Our experiments measuring AQP0 permeability in different lipids are also motivated by the recent finding that the water permeability of another aquaporin (AQP4) strongly depends on bilayer lipid composition and is relatively low in bilayers enriched in cholesterol and SM (Tong et al., 2012). Also, AQP0 aggregation, which occurs in the lens (Costello et al.,1985; Zampighi et al.,1982), acts to partition AQP0 into raft microdomains in bilayers enriched in cholesterol and SM (Tong et al., 2009), which may be relevant to the raft microdomains in the lens (Borchman and Yappert, 2010; Cenedella et al., 2007; Rujoi et al., 2003). Because there have been no reports on AQP0 water permeability reconstituted into bilayers with compositions similar to lens fiber cells, it is unclear how changes in lipid composition that occur with age and region in the lens affect or regulate AQP0 permeability (Borchman and Yappert, 2010).

Another difference between the lens cortex and nucleus is that the cytoplasms of nuclear cells are considerably more acidic than those of the cortex (Mathias et al., 1991). There have been different experimental findings concerning the effect of pH on AQP0 water permeability. Nemeth-Cahalan and Hall (2000) measured a 3.4 fold increase in bovine AQP0 water permeability expressed in Xenopus oocytes, with a lowering of the pH from 7.5 to 6.5, and argued that these results provide evidence for regulation of AQP0 by changes in pH. Varadaraj et al. (2005) also found that decreasing external pH resulted in increased water permeability for AQP0 expressed in Xenopus oocytes, as well as for vesicles formed from cortical fiber cells. We note that in these cortical vesicles there might be contributions from the small amount of AQP5 in the lens (Grey et al., 2013). In contrast, Virkki et al. (2001) found essentially no change in bovine AQP0 water permeability expressed in Xenopus oocytes when the pH was lowered from 7.5 to 6. To distinguish pH effects determined by inherent AQP0 permeability from potential effects of intracellular processes, here we measure AQP0 unit water permeability over the pH range of 7.5–6.5 using proteoliposomes where the AQP0/lipid ratio and exact lipid composition are precisely controlled.

2. Materials and methods

2.1. Materials

The monounsaturated phospholipids palmitoyloleoyl phosphatidylcholine (POPC) {(C16:0)(C18:1)PC} and palmitoyloleoyl phosphatidylglycerol (POPG) {(C16:0)(C18:1)PG}, the fully saturated dipalmitoyl phosphatidylglycerol (DPPG) {(C16:0)(C16:0)PG}, bovine brain sphingomyelin (SM), and cholesterol were purchased from Avanti Polar Lipids (Alabaster, AL). Bovine lenses were from Pel-Freez Biological (Bogers, AR). The detergent n-octyl-D-glucopyranoside (OG) was from Affymetrix (Maumee, OH), the protease inhibitor cocktail, dimethyl sulfoxide (DMSO), and phenylmethylsulphonyl fluoride (PMSF) were obtained from Sigma–Aldrich (St. Louis, MO). Affinity purified rabbit anti-AQP0 was from Chemicon (Billerica, MA) and affinity purified rat anti-AQP5 antibody was from Millipore

(Billerica, MA). SDS-PAGE reagents, Criterion Tris–HCl gel, and nitrocellulose membranes were from Bio-Rad Laboratories (Hercules, CA), and the BCA protein assay was from Thermo Scientific (Rockford, IL).

2.2. Isolation and purification of AQP0

For each preparation, 25 bovine lenses were dissected by removing the epithelial tissue and the cortical tissue was minced into small pieces then homogenized with a Teflon tipped homogenizer in 2 mM EDTA, 2 mM EGTA, and 10 mM HEPES buffer (pH 8) containing a protease inhibitor cocktail. The material was centrifuged for 20 min at 17,000 × *g*, followed by two washes. The resulting crude membrane pellet was diluted in buffer and frozen at −100 °C until further use.

AQP0 was purified following published methods (Gonen et al., 2004a,b; Jarvis and Louis, 1995; Tong et al., 2009). The crude membrane fraction was treated with 3 consecutive washes at 17,000 × *g* in HEPES buffer containing initially 4 M urea, then 7 M urea, and finally 0 M urea. This material was solubilized in 2% OG in buffer, and the insoluble material was removed by centrifugation at 110,000 × *g*. The OG-solubilized supernatant was loaded on a HiTrap Q FF anion exchange column (GE Healthcare, Piscataway, NJ) equilibrated with 1% OG and fractions were eluted with a step gradient of 0 M, 150 mM, 200 mM, and 1 M NaCl in HEPES buffer containing 1% OG. Protein concentrations in the fractions were measured with the BCA assay using a BSA standard (Thermo Scientific, Rockford, IL). The purity of AQP0 was determined by SDS-PAGE and Western blots as we have done previously (Tong et al., 2009). For SDS-PAGE, protein samples were mixed (1:1) with Laemmli sample buffer containing 10% SDS and analyzed with a 4–20% gel. Gels, stained with Sypro Ruby, imaged and analyzed using a BioChemi System with Lab-Works 4.0 (UVP BioImaging System, Upland, CA). Because AQP5, which has a similar molecular weight to AQP0, has been recently demonstrated in lens fiber cells (Grey et al., 2013), Western blotting of the column fractions was also done with an anti-AQP5 primary antibody.

2.3. Reconstitution of AQP0 into proteoliposomes

To obtain bilayers with a range of thicknesses and elastic properties (Tong et al., 2012), we used three specific lipid compositions: (1) a mixture of monounsaturated phospholipids, POPC:-POPG (8:2 M:M); (2) monounsaturated phospholipids with cholesterol, POPC:POPG:cholesterol (4:2:4 M:M:M); and (3) a mixture of SM, a fully saturated phospholipid and cholesterol, SM:DPPG:cholesterol (4:2:4 M:M:M). The negatively charged PGs, with hydrocarbon chain compositions similar to the accompanying choline-containing phospholipids, were included to help stabilize large unilamellar proteoliposomes and minimize aggregation. The lipids were mixed in chloroform:methanol, dried by rotary evaporation, and hydrated in 25 mM HEPES, 50 mM NaCl, 2 mM DTT, 1 mM PMSF at pH 7.5 (buffer A) containing 2% OG. To ensure complete hydration, the SM:DPPG:cholesterol specimens were hydrated at 40 °C, whereas the other lipids were hydrated at 20 °C. The lipids and proteins in OG were mixed at appropriate lipid:protein ratios, OG was removed by dialysis against buffer A, initially for 4 h at room temperature followed by 2 days at room temperature for SM:DPPG:cholesterol or at 4 °C for the other lipids. The resulting lipid:protein vesicles were collected by ultracentrifugation (Tong et al., 2012) and resuspended in dialysis buffer A plus 50 mM sucrose or in buffer B (25 mM MES, 50 mM NaCl, 2 mM DTT, 1 mM PMSF, pH 6.5) plus 50 mM sucrose. Large unilamellar proteoliposomes were obtained by extrusion through 100 nm pore filters (Avanti Polar Lipids, Alabaster, AL). For each sample the average vesicle diameter was determined by quasi-elastic light scattering with a ZetaPlus Zeta Potential Analyzer (Brookhaven Instruments, Holtsville, NY), and ranged from 100 nm to 180 nm depending on the sample

protein/lipid ratio. The AQP0 unit water permeabilities were found to be independent of average vesicle diameter.

The lipid and protein compositions of the extruded proteoliposomes were determined by phosphate assays (Chen et al., 1956) and SDS-PAGE, respectively. AQP0 in proteoliposomes and known amounts of AQP0 in OG (standardized by BCA assay) were analyzed on the same SDS gel. Integrated optical densities were measured, and the absolute AQP0 concentrations in proteoliposomes were calculated by comparison with the standards, which showed a linear response. This SDS-PAGE approach was necessary for the proteoliposomes because the lipids interfered with direct BCA assays.

2.4. Water permeability measurements

Water permeabilities were measured following techniques that apply an osmotic gradient with sucrose solutions and determine as a function of time the change in proteoliposome volume due to water efflux (Borgnia et al.,1999; Liu et al., 2006; Walz et al.,1994; Yukutake et al., 2008; Zeidel et al.,1992, 1994). To measure permeabilities at pH 7.5 or pH 6.5 these sucrose solutions were made using buffer A or buffer B, respectively. We measured the volume change by light scattering with a wavelength of 600 nm (Kai et al., 2010; Tong et al., 2012; Yang et al., 1997) using a SX20 Stopped-Flow Spectrometer (Applied Photophysics, Leatherhead, UK). The proteoliposome permeabilities (p_f), with units of cm/sec, were calculated from the formula

$$p_f = k/\{(\mathrm{SAV})(V_w)(C_{\mathrm{out}} - C_{\mathrm{in}})\} \quad (1)$$

where k is the shrinkage rate determined by exponential fits to the light scattering data, SAV is the vesicle surface area to volume ratio, V_W is the partial molar volume of water (18 cm3/mol), and C_{in} (50 mM) and C_{out} (150 mM) are the initial concentrations of solute inside and outside the vesicles (Borgnia et al., 1999; Kai et al., 2010). For proteoliposomes made from POPC:POPG or POPC:POPG:cholesterol the light scattering data were recorded from 0 to 5 s, whereas for the slower volume changes observed with proteoliposomes containing SM:DPPG:cholesterol data were recorded from 0 to 20 s. The light scattering data were fit using Logger Pro 3.8 (Vernier Software, Beaverton, OR).

The AQP0 single-channel unit permeabilities (P_u), with units of cm^3/sec, were determined with the formula $P_u = p_f/\mathrm{SuD}$ (Werten et al., 2001), where SuD is the AQP-0 density per unit surface area. For each proteoliposome preparation, SuD was calculated from the measured vesicle diameters, protein concentrations, lipid concentrations, and area per lipid molecule (A_m). For our lipid systems A_m was estimated from literature X- ray diffraction and monolayer data as described in detail previously (Tong et al., 2012). For POPC:POPG, POPC:POPG:cholesterol, and SM:DPPG:cholesterol we used A_m = 0.66 nm^2, 0.47 nm^2, and 0.42 nm^2, respectively.

3. Results

Polyacrylamide gels of fractions from the anion exchange columns eluted at 150 mM, 250 mM, and 1 M NaCl all showed bands with an approximate molecular weight of 26 kD. Western blots showed that AQP0 was highly enriched in the column fractions eluted at 150 mM and 200 mM NaCl but not present in appreciable quantities in the 1 M fraction (Tong et al., 2009), whereas AQP5 was located in the column fraction eluted at 1 M NaCl but not in the 150 or 200 mM fractions (data not shown). For these column fractions of OG-soluble bovine lens, PAGE analysis showed that there was about 12 times more AQP0 than AQP5, consistent with proteomics results for the human lens (Grey et al., 2013). For all work

described in this paper we used the column fraction eluted with 150 mM that was enriched in AQP0.

Fig. 1 shows typical time courses of the osmotic gradient-driven changes in light scattering for 4:2:4 POPC:POPG:cholesterol single-walled vesicles in the presence and absence of AQP0. For both traces the light scattering increased sharply after the osmotic gradient was applied at time $t = 0$ s and eventually leveled off. In the absence of protein, the light scattering trace could be fit closely with a single exponential function yielding a single value of shrinkage rate constant (k). For these control vesicles the value of p_f calculated with Eqn. (1) was $3.3 \pm 0.2 \times 10^{-3}$ cm/s (mean ± SEM), which is similar to the value of $2.9 \pm 0.6 \times 10^{-3}$ cm/s previously obtained with the similar lipid system of 6.7:3.3 POPC:cholesterol (Gensure et al., 2006). The presence of AQP0 increased the rate of the change in light scattering (Fig. 1), indicating that AQP0 increased the water permeability of the vesicle.

Representative changes in light scattering are shown in Fig. 2 for proteoliposomes containing similar concentrations of AQP0 in bi-layers of different lipid compositions, with those containing cholesterol designed to mimic membrane compositions found in the lens. The rate of scattering strongly depended on the lipid system, being fastest for POPC:POPG, slower for POPC:POPG:cholesterol, and slowest for SM:DPPG:cholesterol. For each lipid system, the traces could be closely fit with the sum of two exponential functions, yielding two shrinkage rates and two values of p_f, a larger one (k_1) that increased with increasing protein/lipid (P/L) ratio, and a smaller one (k_2) that was independent of P/L and had a similar value to the control liposome. This is illustrated for the SM:DPPG:cholesterol system with the open triangles in Fig. 3. For subsequent analysis with each lipid composition, we used the larger values of p_f (calculated with k_1) that increased with increasing P/L.

Similar experiments were used with Eq (1) to calculate p_f for AQP0 over broad ranges of protein/lipid (P/L) ratios for all three lipid systems at pH 7.5 (Fig. 3). In the absence of AQP0 (P/L = 0) the water permeability for each bilayer system studied here was similar to previously published values for similar lipids (Tong et al., 2012). Upon the addition of AQP0 in all three lipid systems, the proteoliposome water permeability increased linearly with increasing P/L ratio. However, p_f depended strongly on the composition of the lipid bilayer and, for a given protein/lipid ratio, varied in the order POPC:POPG > POPC:POPG:cholesterol > SM:DPPG:cholesterol (Fig. 3).

Using the proteoliposome permeability (p_f) data (Fig. 3) along with the AQP0 density per surface area (SuD) for each proteoliposome, we calculated the single channel (unit) permeability (P_u) for AQP0 at pH 7.5 for the three different lipid systems. As shown in Fig. 4, P_u depended strongly on the composition of the lipid bilayer, with POPC:POPG >POPC:POPG:cholesterol >SM:DPPG:cholesterol.

Next we compared these measured values of P_u to the values determined for AQP4, a major water channel in the brain. In Fig. 5 we show unit water permeabilities for AQP0 and the M1 isoform of AQP4 (from Tong et al. (2012)) for the same 3 lipid systems. Two major points should be noticed. First, for each lipid composition the values of P_u were smaller by about an order of magnitude for AQP0 than for AQP4. Second, for both AQP0 and AQP4 the unit permeability depended strongly on the composition of the bilayer matrix. The addition of 40 mol% cholesterol to PC:PG bilayers significantly reduced the unit permeability for both AQPs, and for both AQPs the values of P_u were smallest in SM:DPPG:cholesterol bilayers.

Measurements of p_f and P_u were also performed at pH 6.5 for proteoliposomes containing cholesterol, as found in the lens nucleus. As shown in Fig. 6, reducing the pH from 7.5 to

6.5 increased the values of P_u by about 30% for PC:PG:cholesterol and about 50% for SM:PG:cholesterol.

Previous work from our laboratory showed that the unit permeability of AQP4 depended on the lipid bilayer composition and properties, specifically on the bilayer hydrocarbon thickness (d_{hc}) and bilayer compressibility modulus (K_A), a measure of bilayer elasticity (Tong et al., 2012). To test if similar relationships also pertain to AQP0, we plot in Fig. 7 the measured values of P_u as a function of bilayer hydrocarbon thickness (d_{hc}) and $K_A^{1/2}$. We use $K_A^{1/2}$ since it has been experimentally shown in the case of one component PC bilayers that elastic bending (k_c) and area compressibility moduli are related to bilayer hydrocarbon thickness (d_{hc}) by the relation $(k_c/K_A)^{1/2} \propto d_{hc}$ (Rawicz et al., 2000). Values of K_A were calculated based on measurements for similar lipid systems (Rawicz et al., 2000, 2008). For POPC:POPG (8:2) we used K_A of the analogous lipid SOPC (Rawicz et al., 2008), for POPC:POPG:-cholesterol (4:2:4) we used the K_A measured for SOPC:cholesterol (1:1) (Rawicz et al., 2008) modified by a correction factor of 0.6 taking into account the difference between SOPC bilayers containing 50 and 40 mol% cholesterol (see Fig. 3 of (Needham and Nunn, 1990)), and for SM:DPPG:cholesterol (4:2:4) we used K_A of SM:cholesterol (1:1) (Rawicz et al., 2008) with the same correction factor of 0.6. The values of d_{hc} were taken from X-ray diffraction data; for POPC:POPG we used d_{hc} measured for POPC (Kucerka et al., 2005), for POPC:POPG:cholesterol we used d_{hc} of SOPC:cholesterol (Pan et al., 2008), and for SM:DPPG:cholesterol we used d_{hc} of SM:cholesterol (Gandhavadi et al., 2002). For AQP0, P_u decreased monotonically with increasing values of either d_{hc} (Fig. 7A) or $K_A^{1/2}$ (Fig. 7B).

4. Discussion

4.1. Proteoliposome permeabilities

There have been several previous measurements of p_f for proteoliposomes containing various AQPs, including AQP1 (Walz et al., 1994; Zeidel et al., 1994), AQP2 (Eto et al., 2010; Werten et al., 2001), AQP4 (Kai et al., 2010; Tong et al., 2012; Yang et al., 1997; Yukutake et al., 2008), AQP8 (Liu et al., 2006), and AQP9 (Carbrey et al., 2003). Many of these experiments used bilayers primarily containing bacterial lipids, although some have been done in phospholipids with smaller concentrations of cholesterol than used here (Yang et al., 1997; Zeidel et al., 1994). The only previous osmotic permeability experiments performed with rigid bilayers containing SM and cholesterol were those of Tong et al. (2012) with AQP4. In the case of AQP0 it is important to determine channel water permeability in bilayers containing high concentrations of SM and cholesterol, as both are major lipid components of lens fiber cell membranes (Borchman and Yappert, 2010; Zelenka, 1984; Zigman et al., 1984).

Relatively few experiments have been performed to determine unit channel permeability (P_u) for AQPs in proteoliposomes. For AQP1, P_u has been determined to be 4.6×10^{-14} cm^3/s in bacterial phospholipids (Zeidel et al., 1994), which is comparable to P_u for AQP0 in PC:PG bilayers, but much larger than P_u for AQP0 in SM:PG:cholesterol bilayers. For AQP4, P_u has been measured in several lipid systems, including DPPC:PE:PI:cholesterol (4.5:2.3:0.5:2.7) (Yang et al., 1997), as well as the same bilayer systems as used in this current paper (Tong et al., 2012) (see Fig. 5). Yang et al. (1997) recorded $P_u = 1.5 \times 10^{-13}$ cm^3/s for AQP4 in their bilayers containing 27% cholesterol, which is between our measured values of $P_u = 3.3 \times 10^{-13}$ cm^3/s in PC:PG bilayers containing no cholesterol and $P_u = 1.2 \pm 0.1 \times 10^{-13}$ cm3/s in PC:PG:cholesterol bilayers containing 40% cholesterol.

To obtain a good fit to our light scattering data it was necessary to use the sum of two exponential functions, which previously has been done for some AQP-containing proteoliposomes (Carbrey et al., 2003; Tong et al., 2012). As previously argued by Tong et al. (2012) for AQP4, the faster exponential rise (k_1) represents water permeability through the AQP0 channel, whereas the slower exponential rise (k_2) is probably due to normal water leakage through the bilayer matrix. Thus, we assert that the two values of k represent two distinct avenues of water flux, one through the AQP0 channel and the second through the surrounding bilayer. In support of this bilayer leakage explanation for the slower exponential rise, we note that for k_2 the p_f values were independent of protein/lipid ratio and similar to control liposomes (Fig. 3), whereas for the faster exponential rise (k_1) the values of p_f increased linearly with increasing protein/lipid ratio. We had found previously in the case of AQP4 that a single exponential function could fit data obtained from cholesterol-containing bilayers where the AQP4 permeability was large compared to that of the matrix bilayer, whereas 2 exponential were needed to give a close fit to the scattering data for more leaky PC:PG bilayers where the bilayer matrix leakage was more comparable to that of the AQP4 permeability (Tong et al., 2012). In the case of AQP0, the unit water permeability is much smaller than that of AQP4 (Fig. 5), so that the permeability of the bilayer is closer to that of the AQP0 channel permeability than it is for AQP4. Therefore, we argue that 2 exponential functions are needed to closely fit the light scattering data for AQP0 incorporated into any bilayer matrix.

4.2. Possible molecular mechanisms for bilayer modification of AQP0 water permeability

We now consider possible mechanisms by which changes in bilayer lipid composition modified the AQP0 single channel permeability (Fig. 7). Both theoretical treatments (Nielsen et al., 1998; Phillips et al., 2009; Wiggins and Phillips, 2005) and experimental studies (Baenziger et al., 2000; Chang et al., 1995; Patel et al., 2001; Schmidt and Mackinnon, 2008) indicate that bilayer structural and elastic properties can affect protein conformation and activity, with the structural and elastic properties being interrelated (Perozo et al., 2002; Rawicz et al., 2008; Yuan et al., 2007). Thus, there is a coupling of the protein to the bilayer hydrophobic core so the bilayer becomes an allosteric regulator of membrane protein function (Lundbaek et al., 2005).

Bilayer width plays a role in protein activity due to “hydrophobic mismatch” between protein hydrophobic length and bilayer hydrocarbon thickness (d_{hc}) (Andersen et al., 2007; Dumas et al., 2000; Hong and Tamm, 2004; Nyholm et al., 2007; Perozo et al., 2002; Pilot et al., 2001; Yuan et al., 2007). A hydrophobic coupling between protein and surrounding bilayer exists due to the high cost of exposing either hydrophobic amino acid residues or lipid acyl chains to the aqueous environment (Andersen et al., 2007; Israelachvili et al., 1977; Nielsen et al., 1998). To avoid this hydrophobic mismatch there is either a change in protein conformation or local bilayer thickness. Experiments have shown that hydrophobic mismatch affects the activity of melibiose transporters (Dumas et al., 2000), BK calcium channels (Yuan et al., 2007), and mechanosensitive ion channels (Perozo et al., 2002).

Crystal structures can be used to obtain information on the hydrophobic length of AQP0. In crystals of AQP0 reconstituted in dimyristoyl phosphatidylcholine (DMPC), the width of the DMPC bilayer is 2.4 nm (Hite et al., 2008), which presumably closely matches the length of the hydrophobic region of AQP0. Also, in crystals of AQP0 in OG, the length of the cylindrical water channel is 2.8 nm (Harries et al., 2004). Both of these measured lengths are closer to d_{hc} for POPC:POPG (2.7 nm) than for POPC:POPG:-cholesterol (3.3 nm) or SM:DPPG:cholesterol (3.6 nm) (Fig. 7A). Thus, for our lipid systems, the “hydrophobic mismatch” between AQP0 hydrophobic length and d_{hc} varies in the order SM:DPPG:cholesterol > POPC:POPG:cholesterol > POPC:POPG, consistent with our observed differences in P_u.

In terms of bilayer elastic properties, Hite et al. (2008) suggest that lateral pressure from lipids surrounding AQP0 could restrict the conformational flexibility of its transmembrane domain. This could help explain the dependence of AQP0 P_u on bilayer composition (Fig. 7B), as the lateral pressure profile depends on bilayer cholesterol content (Cantor, 1999a, b; Samuli Ollila et al., 2007) and phospholipid hydrocarbon chain unsaturation (Cantor, 1997, 1999a, b). Several studies have indicated that the hydrocarbon chains are quite ordered in lens bilayers (Borchman et al., 1999; Borchman and Yappert, 1998; Widomska et al., 2007), particularly in cataractous lenses (Huang et al., 2005). EPR spectra have shown that the relatively large order parameters of calf lens lipids are closer to those of equimolar POPC:cholesterol bilayers than to those of POPC bilayers (Widomska et al., 2007).

Therefore, we argue that small AQP0 transmembrane conformational changes resulting from differences in bilayer thickness (Fig. 7A) or bilayer elastic properties (Fig. 7B) could modify the single-file movement of water molecules through the narrow AQP0 water channel. Future experiments will be designed to determine the relative contributions of bilayer thickness and elasticity on AQP water permeability.

4.3. Implications for roles of AQP0 in lens function

AQP0 is the most abundant transmembrane protein in lens fiber cells. Although this protein is critical to the growth, development, and function of the lens (Francis et al., 2000; Shiels and Bassnett, 1996; Shiels et al., 2001, 2000; Varadaraj et al., 2007; Verkman, 2003), fundamental questions remain concerning AQP0's specific roles. The studies presented here have been designed to provide details on AQP0 water permeability in bilayers containing the major types of lipids found in the lens.

A major observation is that the unit water permeability of AQP0 in SM:cholesterol bilayers is about 7 times smaller than P_u for AQP0 in PC:PG bilayers. This implies that the water permeability of AQP0 in fiber cells in the lens nucleus is quite small, and smaller than P_u for AQP0 in the lens cortex. This information should be useful in testing models (such as those developed by Mathias and colleagues (Donaldson et al., 2001; Mathias et al., 2007)) for the internal circulation of ions within the lens that is coupled to water flow. AQP5 is present throughout bovine and human lenses but its abundance is reduced in deeper regions (Grey et al., 2013). There is considerably more AQP0 than AQP5 in lens fiber cells (Grey et al., 2013). However, the higher permeability of AQP5, at least as determined in Xenopus oocytes (Yang and Verkman, 1997), indicates that AQP5 might modulate water permeability in the lens, an idea that needs to be tested (Grey et al., 2013).

A further consideration in analyzing membrane water flux in the lens is that AQP0 could be sequestered into raft microdomains enriched in SM and cholesterol, where, based on the results of Fig. 4, AQP0 channel permeability should be small. Two factors could be involved in the sorting of AQP0 to rafts. First, it has been demonstrated that AQP0 aggregation or homo-oligomerization brings AQP0 into raft microdomains (Tong et al., 2009). Second, the acylation of AQP0 also promotes raft incorporation (Schey et al., 2010).

Lowering of pH from 7.5 to 6.5 increased the P_u of AQP0 (Fig. 5), although not by as large a factor as found for p_f changes measured in frog oocytes (Nemeth-Cahalan et al., 2013; Nemeth-Cahalan and Hall, 2000). As previously shown, several factors in cells could affect AQP0 permeability, such as phosphorylation (Gold et al., 2012) and interactions with either cytoplasmic (Lindsey Rose et al., 2006; Nakazawa et al., 2011; Nemeth-Cahalan et al., 2004; Reichow and Gonen, 2008; Rose et al., 2008) or extracellular proteins (Liu and Liang, 2008). Our data indicate that an important additional factor to consider is bilayer composition, which modifies inherent AQP0 permeability.

Another possible role for AQP0 in the lens is in cell-to-cell adhesion (Buzhynskyy et al., 2007; Gonen et al., 2004a, b; Kumari and Varadaraj, 2009; Michea et al., 1995). Early freeze-fracture and thin section electron microscopy showed that tight intracellular contacts were found in the lens at the location of square arrays of transmembrane proteins (Costello et al., 1985; Zampighi et al., 1982), now known to be AQP0 (Zampighi et al., 2002). These "thin junctions" (Costello et al., 1985; Zampighi et al., 1982) that collapse the fluid space between adjacent cells could be a factor in minimizing light scattering by the lens (Shiels, 2012). Crystal studies indicate that AQP0 is in a closed form when located in membrane junctions (Engel et al., 2008; Gonen et al., 2004a, b).

4.4. Conclusions

The data presented in this report show that the unit water permeability of AQP0 channels strongly depended on the lipid composition of the membrane bilayer matrix as modified by both cholesterol content and phospholipid hydrocarbon chain constituents. In particular, there was a strong dependence of unit permeability on bilayer thickness and elasticity. Based on the lipid compositions of lens fiber cells these data imply that the unit permeability of AQP0 channels is less in the lens nucleus than in the cortex.

Acknowledgments

We thank Dr. Terrence Oas for use of the stopped-flow apparatus, Dr. David Needham for use of the quasi-elastic light scattering equipment, and Drs. Jennifer Carbrey, Sid Simon, and Joe Corless for many helpful suggestions. This work was supported by grant GM27278 from the National Institutes of Health.

References

Agre P, Kozono D. Aquaporin water channels: molecular mechanisms for human diseases. FEBS Lett. 2003; 555:72–78. [PubMed: 14630322]

Agre P, Preston GM, Smith BL, Jung JS, Raina S, Moon C, Guggino WB, Nielsen S. Aquaporin CHIP: the archetypal molecular water channel. Am J Physiol. 1993; 265:F463–F476. [PubMed: 7694481]

Al-Ghoul KJ, Kirk T, Kuszak AJ, Zoltoski RK, Shiels A, Kuszak JR. Lens structure in MIP-deficient mice. Anat Rec A Discov Mol Cell Evol Biol. 2003; 273:714–730. [PubMed: 12845708]

Andersen OS, Bruno MJ, Sun H, Koeppe RE 2nd. Single-molecule methods for monitoring changes in bilayer elastic properties. Meth Mol Biol. 2007; 400:543–570.

Baenziger JE, Morris ML, Darsaut TE, Ryan SE. Effect of membrane lipid composition on the conformational equilibria of the nicotinic acetylcholine receptor. J Biol Chem. 2000; 275:777–784. [PubMed: 10625607]

Ball LE, Little M, Nowak MW, Garland DL, Crouch RK, Schey KL. Water permeability of C-terminally truncated aquaporin 0 (AQP0 1-243) observed in the aging human lens. Invest Ophthalmol Vis Sci. 2003; 44:4820–4828. [PubMed: 14578404]

Borchman D, Cenedella RJ, Lamba OP. Role of cholesterol in the structural order of lens membrane lipids. Exp Eye Res. 1996; 62:191–197. [PubMed: 8698079]

Borchman D, Tang D, Yappert MC. Lipid composition, membrane structure relationships in lens and muscle sarcoplasmic reticulum membranes. Bio-spectroscopy. 1999; 5:151–167.

Borchman D, Yappert MC. Age-related lipid oxidation in human lenses. Invest Ophthalmol Vis Sci. 1998; 39:1053–1058. [PubMed: 9579487]

Borchman D, Yappert MC. Lipids and the ocular lens. J Lipid Res. 2010; 51:2473– 2488. [PubMed: 20407021]

Borchman D, Yappert MC, Afzal M. Lens lipids and maximum lifespan. Exp Eye Res. 2004; 79:761–768. [PubMed: 15642313]

Borgnia MJ, Kozono D, Calamita G, Maloney PC, Agre P. Functional reconstitution and characterization of AqpZ, the E. coli water channel protein. J Mol Biol. 1999; 291:1169–1179. [PubMed: 10518952]

Buzhynskyy N, Hite RK, Walz T, Scheuring S. The supramolecular architecture of junctional microdomains in native lens membranes. EMBO Rep. 2007; 8:51–55. [PubMed: 17124511]

Cantor RS. The lateral pressure profile in membranes: a physical mechanism of general anesthesia. Biochemistry. 1997; 36:2340–2343.

Cantor RS. The influence of membrane lateral pressures on simple geometric models of protein conformational equilibria. Chem Phys Lipids. 1999a; 101:45–56. [PubMed: 10810924]

Cantor RS. Lipid composition and the lateral pressure profile in bilayers. Biophys J. 1999b; 76:2625–2639. [PubMed: 10233077]

Carbrey JM, Gorelick-Feldman DA, Kozono D, Praetorius J, Nielsen S, Agre P. Aquaglyceroporin AQP9: solute permeation and metabolic control of expression in liver. Proc Natl Acad Sci U S A. 2003; 100:2945–2950. [PubMed: 12594337]

Cenedella RJ, Sexton PS, Brako L, Lo WK, Jacob RF. Status of caveolin-1 in various membrane domains of the bovine lens. Exp Eye Res. 2007; 85:473–481. [PubMed: 17669400]

Chandy G, Zampighi GA, Kreman M, Hall JE. Comparison of the water transporting properties of MIP and AQP1. J Membr Biol. 1997; 159:29–39. [PubMed: 9309208]

Chang HM, Reitstetter R, Mason RP, Gruener R. Attenuation of channel kinetics and conductance by cholesterol: an interpretation using structural stress as a unifying concept. J Membr Biol. 1995; 143:51–63. [PubMed: 7714888]

Chen PS Jr, Toribara TY, Warner H. Microdetermination of phosphorous. Anal Chem. 1956; 28:1756–1758.

Costello MJ, McIntosh TJ, Robertson JD. Membrane specializations in mammalian lens fiber cells: distribution of square arrays. Curr Eye Res. 1985; 4:1183–1201. [PubMed: 4075818]

Deeley JM, Mitchell TW, Wei X, Korth J, Nealon JR, Blanksby SJ, Truscott RJ. Human lens lipids differ markedly from those of commonly used experimental animals. Biochim Biophys Acta. 2008; 1781:288–298. [PubMed: 18474264]

Donaldson P, Kistler J, Mathias RT. Molecular solutions to mammalian lens transparency. News Physiol Sci. 2001; 16:118–123. [PubMed: 11443230]

Donaldson PJ, Chee KS, Lim JC, Webb KF. Regulation of lens volume: implications for lens transparency. Exp Eye Res. 2009; 88:144–150. [PubMed: 19091312]

Dumas F, Tocanne JF, Leblanc G, Lebrun MC. Consequences of hydrophobic mismatch between lipids and melibiose permease on melibiose transport. Biochemistry. 2000; 39:4846–4854. [PubMed: 10769142]

Engel A, Fujiyoshi Y, Gonen T, Walz T. Junction-forming aquaporins. Curr Opin Struct Biol. 2008; 18:229–235. [PubMed: 18194855]

Estrada R, Yappert MC. Alternative approaches for the detection of various phospholipid classes by matrix-assisted laser desorption/ionization time-of-flight mass spectrometry. J Mass Spectrom. 2004; 39:412–422. [PubMed: 15103655]

Eto K, Noda Y, Horikawa S, Uchida S, Sasaki S. Phosphorylation of aquaporin-2 regulates its water permeability. J Biol Chem. 2010; 285:40777–40784. [PubMed: 20971851]

Francis P, Chung JJ, Yasui M, Berry V, Moore A, Wyatt MK, Wistow G, Bhattacharya SS, Agre P. Functional impairment of lens aquaporin in two families with dominantly inherited cataracts. Hum Mol Genet. 2000; 9:2329–2334. [PubMed: 11001937]

Gandhavadi M, Allende D, Vidal A, Simon SA, McIntosh TJ. Structure, composition, and peptide binding properties of detergent soluble bilayers and detergent resistant rafts. Biophys J. 2002; 82:1469–1482. [PubMed: 11867462]

Gensure RH, Zeidel ML, Hill WG. Lipid raft components cholesterol and sphingomyelin increase H+/OH− permeability of phosphatidylcholine membranes. Biochem J. 2006; 398:485–495. [PubMed: 16706750]

Gold MG, Reichow SL, O'Neill SE, Weisbrod CR, Langeberg LK, Bruce JE, Gonen T, Scott JD. AKAP2 anchors PKA with aquaporin-0 to support ocular lens transparency. EMBO Mol Med. 2012; 4:15–26. [PubMed: 22095752]

Gonen T, Cheng Y, Kistler J, Walz T. Aquaporin-0 membrane junctions form upon proteolytic cleavage. J Mol Biol. 2004a; 342:1337–1345. [PubMed: 15351655]

Gonen T, Sliz P, Kistler J, Cheng Y, Walz T. Aquaporin-0 membrane junctions reveal the structure of a closed water pore. Nature. 2004b; 429:193–197. [PubMed: 15141214]

Grey AC, Walker KL, Petrova RS, Han J, Wilmarth PA, David LL, Donaldson PJ, Schey KL. Verification and spatial localization of aquaporin-5 in the ocular lens. Exp Eye Res. 2013; 108:94–102. [PubMed: 23313152]

Harries WE, Akhavan D, Miercke LJ, Khademi S, Stroud RM. The channel architecture of aquaporin 0 at a 2.2-A resolution. Proc Natl Acad Sci U S A. 2004; 101:14045–14050. [PubMed: 15377788]

Hill WG, Southern NM, MacIver B, Potter E, Apodaca G, Smith CP, Zeidel ML. Isolation and characterization of the Xenopus oocyte plasma membrane: a new method for studying activity of water and solute transporters. Am J Physiology-Renal Physiol. 2005; 289:F217–F224.

Hite RK, Gonen T, Harrison SC, Walz T. Interactions of lipids with aquaporin-0 and other membrane proteins. Pflugers Archiv. 2008; 456:651–661. [PubMed: 17932686]

Hong H, Tamm LK. Elastic coupling of integral membrane protein stability to lipid bilayer forces. Proc Natl Acad Sci U S A. 2004; 101:4065–4070. [PubMed: 14990786]

Huang L, Grami V, Marrero Y, Tang D, Yappert MC, Rasi V, Borchman D. Human lens phospholipid changes with age and cataract. Invest Ophthalmol Vis Sci. 2005; 46:1682–1689. [PubMed: 15851569]

Israelachvili JN, Mitchell J, Ninham BW. Theory of self-assembly of lipid bilayers and vesicles. Biochim Biophys Acta. 1977; 470:185–201. [PubMed: 911827]

Jarvis LJ, Louis CF. Purification and oligomeric state of the major lens fiber cell membrane proteins. Curr Eye Res. 1995; 14:799–808. [PubMed: 8529419]

Kai L, Kaldenhoff R, Lian J, Zhu X, Dotsch V, Bernhard F, Cen P, Xu Z. Preparative scale production of functional mouse aquaporin 4 using different cell-free expression modes. PLoS One. 2010; 5:e12972. [PubMed: 20885983]

Kucerka N, Tristram-Nagle S, Nagle JF. Structure of fully hydrated fluid phase lipid bilayers with monounsaturated chains. J Membr Biol. 2005; 208:193–202. [PubMed: 16604469]

Kuikka M, Ramstedt B, Ohvo-Rekila H, Tuuf J, Slotte JP. Membrane properties of D-erythro-N-acyl sphingomyelins and their corresponding dihy-dro species. Biophys J. 2001; 80:2327–2337. [PubMed: 11325733]

Kumari SS, Varadaraj K. Intact AQP0 performs cell-to-cell adhesion. Biochem Biophys Res Commun. 2009; 390:1034–1039. [PubMed: 19857466]

Lamba OP, Borchman D, Garner WH. Infrared study of the structure and composition of rabbit lens membranes: a comparative analysis of the lipids of the nucleus, cortex and epithelium. Exp Eye Res. 1993; 57:1–12. [PubMed: 8405165]

Li LK, So L, Spector A. Membrane cholesterol and phospholipid in consecutive concentric sections of human lenses. J Lipid Res. 1985; 26:600–609. [PubMed: 4020298]

Li LK, So L, Spector A. Age-dependent changes in the distribution and concentration of human lens cholesterol and phospholipids. Biochim Biophys Acta. 1987; 917:112–120. [PubMed: 3790601]

Lindsey Rose KM, Gourdie RG, Prescott AR, Quinlan RA, Crouch RK, Schey KL. The C terminus of lens aquaporin 0 interacts with the cyto-skeletal proteins filensin and CP49. Invest Ophthalmol Vis Sci. 2006; 47:1562–1570. [PubMed: 16565393]

Liu BF, Liang JJ. Confocal fluorescence microscopy study of interaction between lens MIP26/AQP0 and crystallins in living cells. J Cell Biochem. 2008; 104:51–58. [PubMed: 18004741]

Liu K, Nagase H, Huang CG, Calamita G, Agre P. Purification and functional characterization of aquaporin-8. Biol Cell. 2006; 98:153–161. [PubMed: 15948717]

Lundbaek J, Birn P, Tape SE, Toombes GE, Søggard R, Koeppe RE, Gruner SM, Hansen AJ, Andersen OS. Capsaicin regulates voltage-dependent sodium channels by altering lipid bilayer elasticity. Mol Pharma-col. 2005; 68:680–689.

Mathias RT, Kistler J, Donaldson P. The lens circulation. J Membr Biol. 2007; 216:1–16. [PubMed: 17568975]

Mathias RT, Riquelme G, Rae JL. Cell to cell communication and pH in the frog lens. J Gen Physiol. 1991; 98:1085–1103. [PubMed: 1783895]

Michea LF, Andrinolo D, Ceppi H, Lagos N. Biochemical evidence for adhesion-promoting role of major intrinsic protein isolated from both normal and cataractous human lenses. Exp Eye Res. 1995; 61:293–301. [PubMed: 7556493]

Mulders SM, Preston GM, Deen PM, Guggino WB, van Os CH, Agre P. Water channel properties of major intrinsic protein of lens. J Biol Chem. 1995; 270:9010–9016. [PubMed: 7536742]

Nakazawa Y, Oka M, Furuki K, Mitsuishi A, Nakashima E, Takehana M. The effect of the interaction between aquaporin 0 (AQP0) and the filensin tail region on AQP0 water permeability. Mol Vis. 2011; 17:3191–3199. [PubMed: 22194645]

Needham D, Nunn RS. Elastic deformation and failure of lipid bilayer membranes containing cholesterol. Biophys J. 1990; 58:997–1009. [PubMed: 2249000]

Nemeth-Cahalan KL, Clemens DM, Hall JE. Regulation of water permeability in enhanced by cooperativity. J Gen Phys. 2013; 141:287–295.

Nemeth-Cahalan KL, Hall JE. pH and calcium regulate the water permeability of aquaporin 0. J Biol Chem. 2000; 275:6777–6782. [PubMed: 10702234]

Nemeth-Cahalan KL, Kalman K, Hall JE. Molecular basis of pH and Ca2+ regulation of aquaporin water permeability. J Gen Physiol. 2004; 123:573–580. [PubMed: 15078916]

Nielsen C, Goulian M, Andersen OS. Energetics of inclusion-induced bilayer deformations. Biophys J. 1998; 74:1966–1983. [PubMed: 9545056]

Nyholm TK, Ozdirekcan S, Killian JA. How protein transmembrane segments sense the lipid environment. Biochemistry. 2007; 46:1457–1465. [PubMed: 17279611]

Pan J, Tristram-Nagle S, Kucerka N, Nagle JF. Temperature dependence of structure, bending rigidity, and bilayer interactions of dioleoylphosphatidylcholine bilayers. Biophys J. 2008; 94:117–124. [PubMed: 17827241]

Patel AJ, Lazdunski M, Honore E. Lipid and mechano-gated 2P domain K(+) channels. Curr Opin Cell Biol. 2001; 13:422–428. [PubMed: 11454447]

Perozo E, Kloda A, Cortes DM, Martinac B. Physical principles underlying the transduction of bilayer deformation forces during mechano sensitive channel gating. Nat Struct Biol. 2002; 9:696–703. [PubMed: 12172537]

Phillips R, Ursell T, Wiggins P, Sens P. Emerging roles for lipids in shaping membrane-protein function. Nature. 2009; 459:379–385. [PubMed: 19458714]

Pilot JD, East JM, Lee AG. Effects of bilayer thickness on the activity of diacylglycerol kinase of Escherichia coli. Biochemistry. 2001; 40:8188–8195. [PubMed: 11444964]

Rawicz W, Olbrich KC, McIntosh T, Needham D, Evans E. Effect of chain length and unsaturation on elasticity of lipid bilayers. Biophys J. 2000; 79:328–339. [PubMed: 10866959]

Rawicz W, Smith BA, McIntosh TJ, Simon SA, Evans E. Elasticity, strength, and water permeability of bilayers that contain raft microdomain-forming lipids. Biophys J. 2008; 94:4725–4736. [PubMed: 18339739]

Reichow SL, Gonen T. Noncanonical binding of calmodulin to aquaporin-0: implications for channel regulation. Structure. 2008; 16:1389–1398. [PubMed: 18786401]

Rose KM, Wang Z, Magrath GN, Hazard ES, Hildebrandt JD, Schey KL. Aquaporin 0-calmodulin interaction and the effect of aquaporin 0 phosphorylation. Biochemistry. 2008; 47:339–347. [PubMed: 18081321]

Rujoi M, Jin J, Borchman D, Tang D, Yappert MC. Isolation and lipid characterization of cholesterol-enriched fractions in cortical and nuclear human lens fibers. Invest Ophthalmol Vis Sci. 2003; 44:1634–1642. [PubMed: 12657603]

Samuli Ollila OH, Rog T, Karttunen M, Vattulainen I. Role of sterol type on lateral pressure profiles of lipid membranes affecting membrane protein functionality: comparison between cholesterol, desmosterol, 7-dehydrocholesterol and ketosterol. J Struct Biol. 2007; 159:311–323. [PubMed: 17369050]

Schey KL, Gutierrez DB, Wang Z, Wei J, Grey AC. Novel fatty acid acylation of lens integral membrane protein aquaporin-0. Biochemistry. 2010; 49:9858–9865. [PubMed: 20942504]

Schmidt D, Mackinnon R. Voltage-dependent K+ channel gating and voltage sensor toxin sensitivity depend on the mechanical state of the lipid membrane. Proc Natl Acad Sci U S A. 2008; 105:19276–19281. [PubMed: 19050073]

Shiels A. Focus on Molecules: major intrinsic protein. Exp Eye Res. 2012; 101:107– 108. [PubMed: 21134370]

Shiels A, Bassnett S. Mutations in the founder of the MIP gene family underlie cataract development in the mouse. Nat Genet. 1996; 12:212–215. [PubMed: 8563764]

Shiels A, Bassnett S, Varadaraj K, Mathias R, Al-Ghoul K, Kuszak J, Donoviel D, Lilleberg S, Friedrich G, Zambrowicz B. Optical dysfunction of the crystalline lens in aquaporin-0-deficient mice. Physiol Genomics. 2001; 7:179–186. [PubMed: 11773604]

Shiels A, Mackay D, Bassnett S, Al-Ghoul K, Kuszak J. Disruption of lens fiber cell architecture in mice expressing a chimeric AQP0-LTR protein. Faseb J. 2000; 14:2207–2212. [PubMed: 11053241]

Tong J, Briggs MM, McIntosh TJ. Water permeability of aquaporin-4 channel depends on bilayer composition, thickness, and elasticity. Biophys J. 2012:103.

Tong J, Briggs MM, Mlaver D, Vidal A, McIntosh TJ. Sorting of lens aquaporins and connexins into raft and nonraft bilayers: role of protein homo-oligomerization. Biophys J. 2009; 97:2493–2502. [PubMed: 19883592]

Varadaraj K, Kumari S, Shiels A, Mathias RT. Regulation of aquaporin water permeability in the lens. Invest Ophthalmol Vis Sci. 2005; 46:1393–1402. [PubMed: 15790907]

Varadaraj K, Kumari SS, Mathias RT. Functional expression of aquaporins in embryonic, postnatal, and adult mouse lenses. Dev Dyn. 2007; 236:1319–1328. [PubMed: 17377981]

Varadaraj K, Kumari SS, Patil R, Wax MB, Mathias RT. Functional characterization of a human aquaporin 0 mutation that leads to a congenital dominant lens cataract. Exp Eye Res. 2008; 87:9–21. [PubMed: 18501347]

Varadaraj K, Kushmerick C, Baldo GJ, Bassnett S, Shiels A, Mathias RT. The role of MIP in lens fiber cell membrane transport. J Membr Biol. 1999; 170:191–203. [PubMed: 10441663]

Verkman AS. Role of aquaporin water channels in eye function. Exp Eye Res. 2003; 76:137–143. [PubMed: 12565800]

Verkman AS, Ruiz-Ederra J, Levin MH. Functions of aquaporins in the eye. Prog Retin Eye Res. 2008; 27:420–433. [PubMed: 18501660]

Virkki LV, Cooper GJ, Boron WF. Cloning and functional expression of an MIP (AQP0) homolog from killifish (Fundulus heteroclitus) lens. Am J Physiol Regul Integr Comp Physiol. 2001; 281:R1994–R2003. [PubMed: 11705786]

Walz T, Smith BL, Zeidel ML, Engel A, Agre P. Biologically active two-dimensional crystals of aquaporin CHIP. J Biol Chem. 1994; 269:1583–1586. [PubMed: 8294400]

Werten PJ, Hasler L, Koenderink JB, Klaassen CH, de Grip WJ, Engel A, Deen PM. Large-scale purification of functional recombinant human aquaporin-2. FEBS Lett. 2001; 504:200–205. [PubMed: 11532454]

Widomska J, Raguz M, Dillon J, Gaillard ER, Subczynski WK. Physical properties of the lipid bilayer membrane made of calf lens lipids: EPR spin labeling studies. Biochim Biophys Acta-biomembr. 2007; 1768:1454–1465.

Wiggins P, Phillips R. Membrane-protein interactions in mechanosensitive channels. Biophys J. 2005; 88:880–902. [PubMed: 15542561]

Yang B, van Hoek AN, Verkman AS. Very high single channel water permeability of aquaporin-4 in baculovirus-infected insect cells and liposomes reconstituted with purified aquaporin-4. Biochemistry. 1997; 36:7625–7632. [PubMed: 9200715]

Yang B, Verkman AS. Water and glycerol permeabilities of aquaporins 1–5 and MIP determined quantitatively by expression of epitope-tagged constructs in Xenopus oocytes. J Biol Chem. 1997; 272:16140–16146. [PubMed: 9195910]

Yappert MC, Borchman D. Sphingolipids in human lens membranes: an update on their composition and possible biological implications. Chem Phys Lipids. 2004; 129:1–20. [PubMed: 14998723]

Yappert MC, Rujoi M, Borchman D, Vorobyov I, Estrada R. Glycero-versus sphingo-phospholipids: correlations with human and non-human mammalian lens growth. Exp Eye Res. 2003; 76:725–734. [PubMed: 12742355]

Yuan C, O'Connell RJ, Jacob RF, Mason RP, Treistman SN. Regulation of the gating of BKCa channel by lipid bilayer thickness. J Biol Chem. 2007; 282:7276–7286. [PubMed: 17209047]

Yukutake Y, Tsuji S, Hirano Y, Adachi T, Takahashi T, Fujihara K, Agre P, Yasui M, Suematsu M. Mercury chloride decreases the water permeability of aquaporin-4-reconstituted proteoliposomes. Biol Cell. 2008; 100:355–363. [PubMed: 18167118]

Zampighi G, Simon SA, Robertson JD, McIntosh TJ, Costello MJ. On the structural organization of isolated bovine lens fiber junctions. J Cell Biol. 1982; 93:175–189. [PubMed: 7068755]

Zampighi GA, Eskandari S, Hall JE, Zampighi L, Kreman M. Micro-domains of AQP0 in lens equatorial fibers. Exp Eye Res. 2002; 75:505–519. [PubMed: 12457863]

Zeidel ML, Ambudkar SV, Smith BL, Agre P. Reconstitution of functional water channels in liposomes containing purified red cell CHIP28 protein. Biochemistry. 1992; 31:7436–7440. [PubMed: 1510932]

Zeidel ML, Nielsen S, Smith BL, Ambudkar SV, Maunsbach AB, Agre P. Ultrastructure, pharmacologic inhibition, and transport selectivity of aquaporin channel-forming integral protein in proteoliposomes. Biochemistry. 1994; 33:1606–1615. [PubMed: 8312280]

Zelenka PS. Lens lipids. Curr Eye Res. 1984; 3:1337–1359. [PubMed: 6391828]

Zigman S, Paxhia T, Marinetti G, Girsch S. Lipids of human lens fiber cell membranes. Curr Eye Res. 1984; 3:887–896. [PubMed: 6467965]

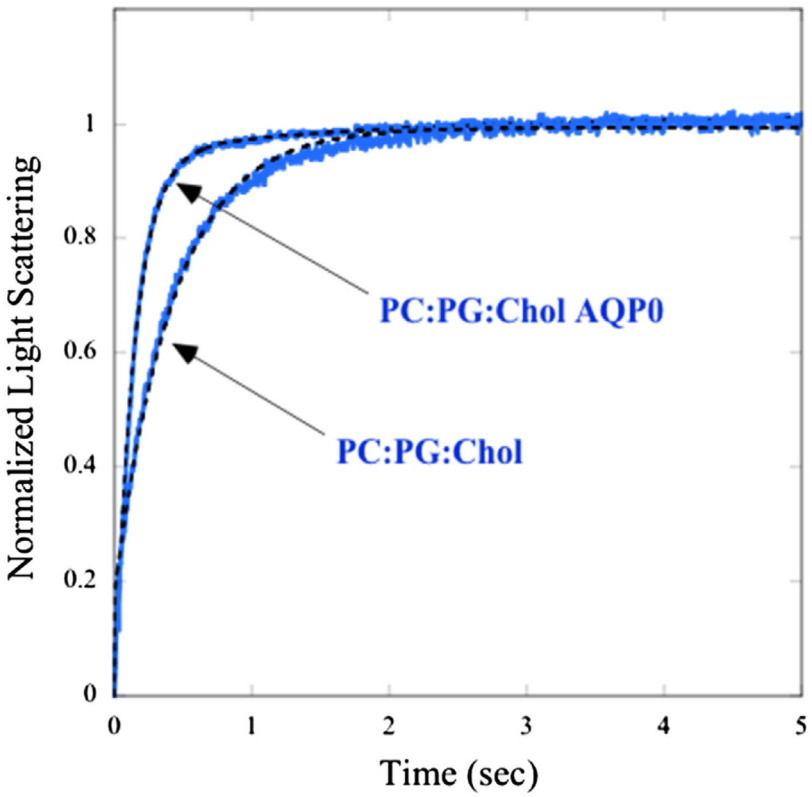

Fig. 1.

Osmotic gradient-driven changes in light scattering for POPC:POPG:cholesterol bilayers without protein or in the presence of AQP0 at a protein/lipid molar ratio of 0.002. For both systems, the osmotic gradient was applied at $t = 0$ and the traces were graphed on the same relative scale by normalizing the light scattering to go from 0 at $t = 0$ to +1 when the scattering plateaued. Fits to the data (single-exponential in the absence of AQP0 and double-exponential in the presence of AQP0) are shown as dotted black lines. With and without AQP0 the fits to the data gave root mean square errors (RMSE) <0.005.

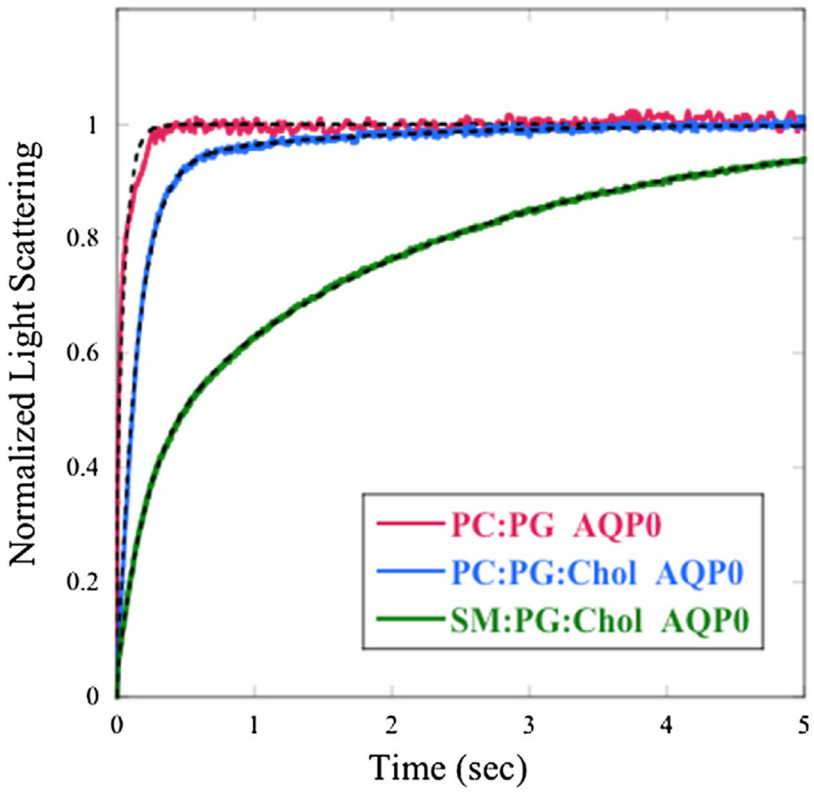

Fig. 2.

Traces of osmotic gradient-driven changes in light scattering for proteoliposomes containing AQP0 at similar protein/lipid (P/L) molar ratios: POPC:POPG (P/ L = 0.002) (red), POPC:POPG:cholesterol (P/L = 0.002) (blue), and SM:DPPG:cholesterol (P/L = 0.003) (green). The light scattering traces were normalized as in Fig. 1. Although data were recorded for a 20-s time period in order for the SM:DPPG:cholesterol trace to plateau, the light-scattering data are displayed for only the first five seconds to better show the differences among the three lipid systems. Double-exponential fits to the data are shown as dotted black lines with fits to all data sets in this paper giving RMSE <0.005.

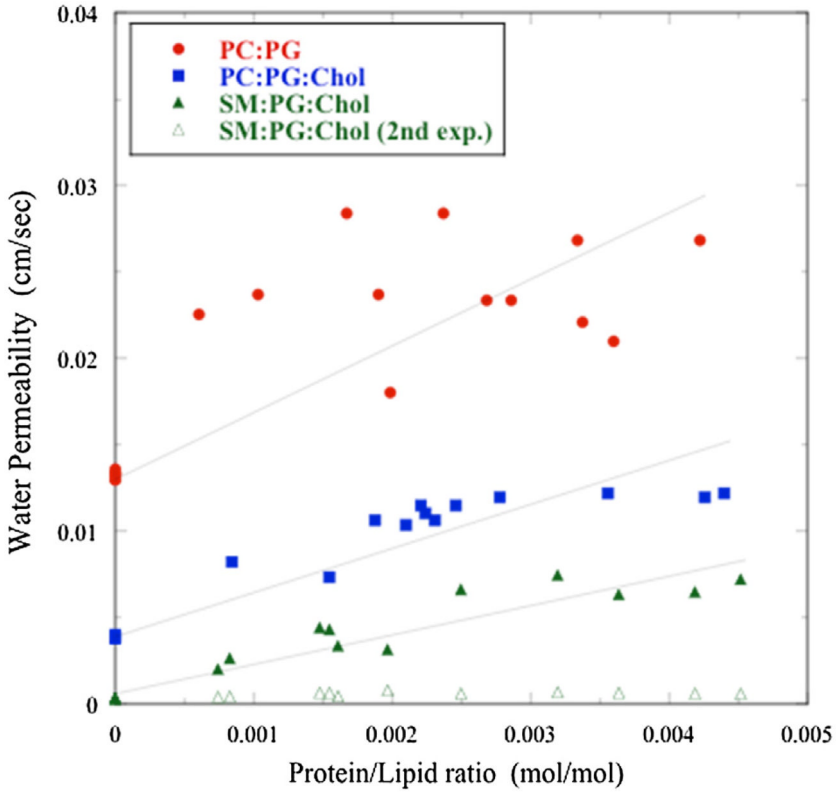

Fig. 3.

Plot of proteoliposome permeability (p_f) as a function of molar protein/lipid (P/L) ratio for AQP0 in bilayers composed of POPC:POPG (red circles), POPC:POPG:-cholesterol (blue squares), and SM:DPPG:cholesterol (green triangles). For each lipid composition fits to the osmotic gradient-driven traces (Fig. 2) yielded two shrinkage rates, with k_1 giving values of p_f that increased linearly with increasing values of P/L (solid symbols), and k_2 giving values of p_f that were nearly independent of P/L (open green triangles show these values for SM:DPPG:cholesterol).

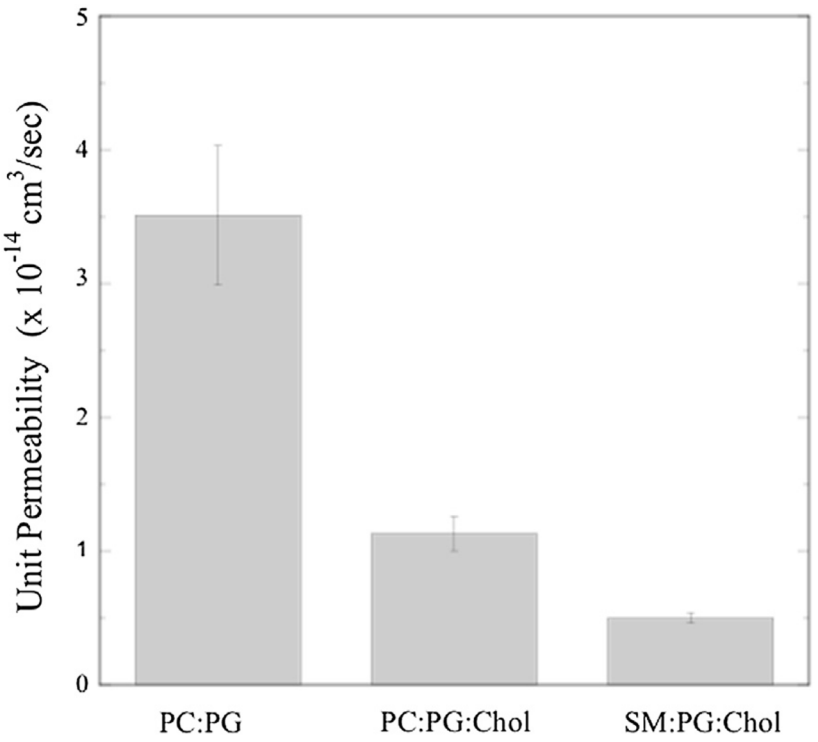

Fig. 4.

Single-channel (unit) permeabilities for AQP0 for bilayers composed of POPC:POPG, POPC:POPG:cholesterol, and SM:DPPG:cholesterol obtained at pH 7.5. (For simplicity, the lipid labels on the *x*-axis do not include the relevant PG.)

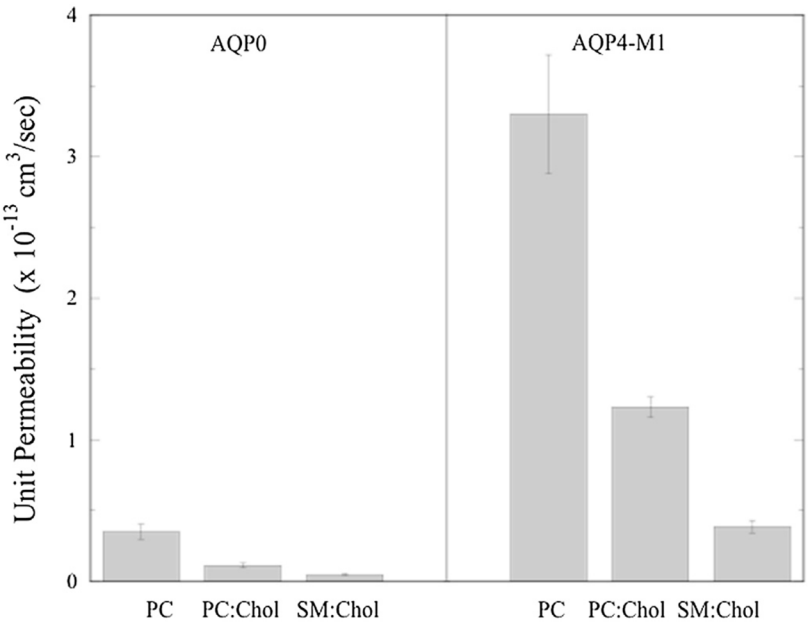

Fig. 5.

Single-channel (unit) permeabilities for AQP0 and AQP4-M1 isoform in bilayers composed of POPC:POPG, POPC:POPG:cholesterol, and SM:DPPG:cholesterol at pH 7.5. The AQP4-M1 data are taken from Tong et al. (2012).

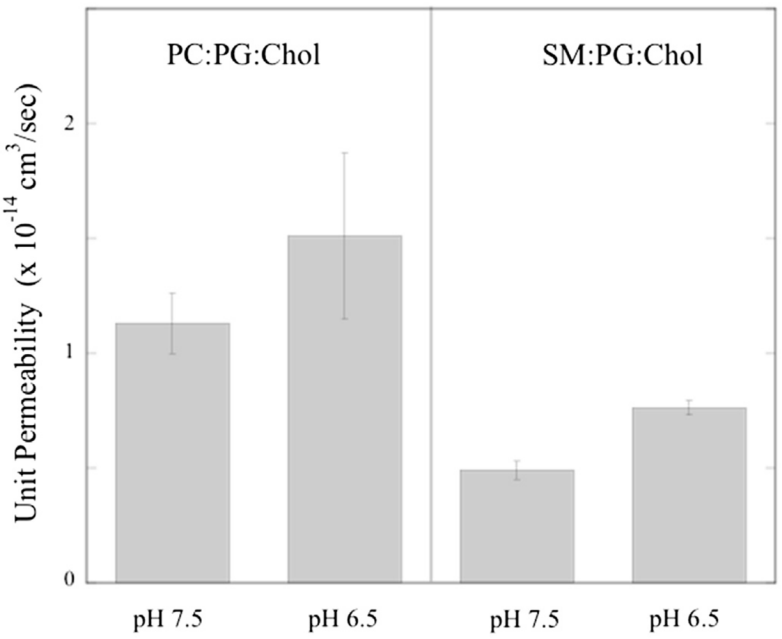

Fig. 6.
Single-channel (unit) permeabilities for AQP0 in bilayers composed of POPC:-POPG:cholesterol and SM:DPPG:cholesterol at pH 7.5 and at pH 6.5.

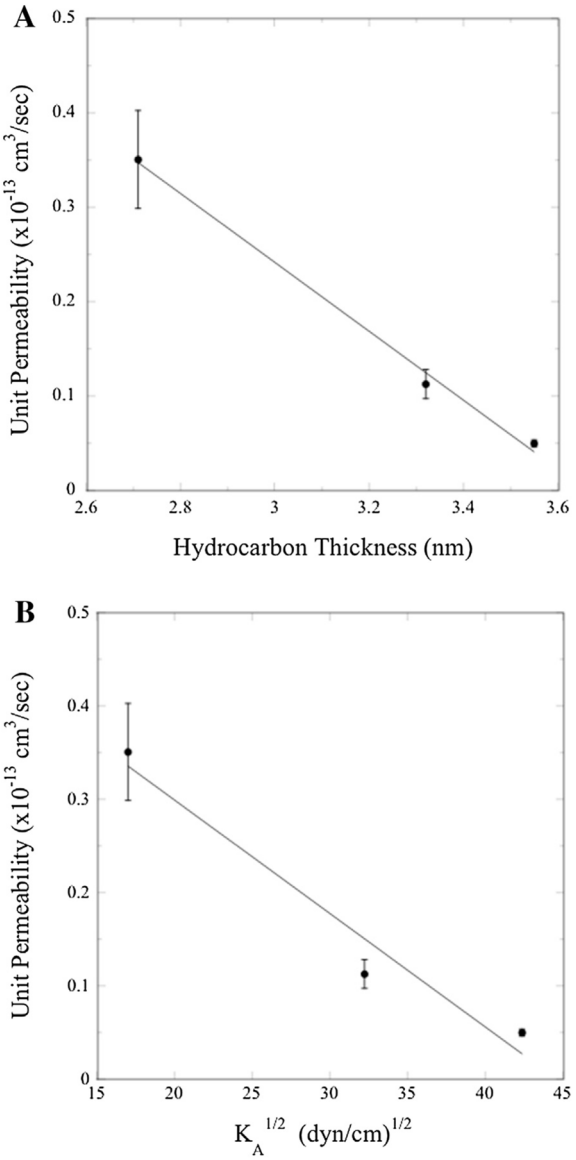

Fig. 7.

Single-channel (unit) water permeabilities at pH 7.5 for AQP0 in bilayers composed of POPC:POPG, POPC:POPG:cholesterol, and SM:DPPG:cholesterol plotted as a function of (**A**) bilayer hydrocarbon thickness and (**B**) the square-root of bilayer area compressibility modulus ($K_A^{1/2}$). Linear fits to the data are shown to guide the eye.